Is the inverse problem technique appropriate for structural health assessment?

Achintya Haldar

University of Arizona, Tucson, AZ 85721, USA

Structural health assessment techniques using system identification-based approaches have recently generated a considerable amount of multidisciplinary research interest. However, in 1979, it was stated that the inverse transformation technique could not identify a system with measured response information. Presence of many sources of error including noise, high frequency content, slope, DC bias, etc. in the measured response information were considered to be the major reasons. However, removing these sources from the measured responses may not be adequate to eliminate the non-convergence problem. In this article, it is conclusively demonstrated that a system can be identified if the amplitude and phase shift errors embedded in the measured responses are mitigated properly. The noise may not be the primary reason for the non-convergence. The conclusions made here are primarily based on the analytical and experimental works completed by the author and his team. Their experience indicates that the system identification-based structural health assessment techniques have unlimited application potential.

Keywords: Experimental verification, finite element method, structural health assessment, system identification, time domain technique.

Introduction

STRUCTURAL health assessment has become one of the major multidisciplinary research areas in engineering. One of the attractive concepts to assess structural health has been the system identification (SI)-based approaches. It is essentially based on the concept that by measuring dynamic excitation and response information, the structural dynamic properties or in most cases stiffness properties of elements can be estimated using the inverse transformation technique. The system is generally represented by the finite element method. By tracking the changes in the stiffness properties if periodic testing were conducted, or by studying the difference in the stiffness properties from expected values obtained from the design drawings, or by simply observing non-uniform or abnormal stiffness properties of elements, the location(s) and the amount of degradation can be established. However, the successes of such approaches have been non-uniform, particularly when measured response information is used to identify systems, and some critics openly stated that it could not be done. They suggested that the presence of noise in the measured response information was the major reason for such failure.

The above statement is in line with the comments made by Maybeck[1] in 1979. According to him 'There are three basic reasons why deterministic system and control theories do not provide a totally sufficient means of performing this analysis and design'. He correctly identified three basic reasons. They are: (1) no mathematical system model is perfect; there are many sources of uncertainty, (2) the disturbances in dynamic systems can neither be controlled nor modelled deterministically, and (3) sensors do not provide perfect and complete data about a system. Since most basic system identification-based approaches fail to consider uncertainty in the formulation, their appropriateness in the structural health assessment is expected to be limited.

The author and his research team faced similar problems in the process of developing a system identification-based nondestructive structural health assessment technique. The method is known as the Generalized Iterative Least Squares – Extended Kalman Filter – with Unknown Input (GILS-EKF-UI) method[2–5]. It is essentially a finite element-based time domain SI technique. The unique feature of the method is that it can identify a system with limited measured noise-contaminated acceleration time histories without using any information on the excitation information. It is based on the Kalman filter approach[6]. To implement the concept, a two-stage substructure approach is used. In the first phase, a substructure is selected that satisfies all the requirements of the MILS-UI procedure[7] which was developed earlier by the author and his team. The first phase generates information on the initial state vector and the input excitation required to implement any EKF-based procedure. In the second stage, the EKF with Weighted Global Iteration (EKF-WGI)[7] is applied to identify the whole structure. This way the whole structure, defect-free or defective, can be identified with limited response measurements in the presence of uncertainty and without using excitation information. However, before the development of the GILS-EKF-UI, it underwent several development phases[8–11]. The research team also experienced the issues

e-mail: haldar@email.arizona.edu

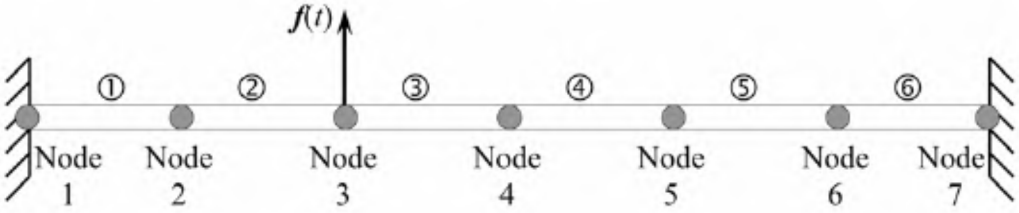

Figure 1. Finite element representation of the beam.

Table 1. Identified modulus of rigidity using computer generated response information

	Undamaged beam		Damaged beam	
Element no.	Identified modulus of rigidity (EI) (Nm^2)	Predicted/theoretical EI = 160.3 (in per cent)	Identified modulus of rigidity (EI) (Nm^2)	Predicted/theoretical EI = 160.3 (in per cent)
1	158.3	98.8	99.5	61.0
2	160.8	100.3	74.1	46.2
3	158.8	99.0	150.6	93.9
4	158.8	99.0	150.6	93.9
5	161.4	100.6	148.6	92.7
6	158.7	99.0	153.3	96.6

raised by Maybeck. However, they successfully mitigated the issues and successfully identified systems using measured response information. The techniques they used to mitigate the issues are presented in detail and the theoretical concept of the GILS-EKF-UI method is briefly discussed here. The details of the theoretical concept can be found elsewhere[2–4].

Structural health assessment has become an active research area in the profession and has attracted multidisciplinary interest. It is impossible to cite all related works in this article. Analytical and experimental works completed by the author and his team are emphasized in the reference section. However, in a recent doctoral thesis, Nasrellah[12] gave an excellent overview of the state of the art. Some of the important review papers that will be of interest to the readers are listed in the reference section of this paper[13–15] for ready reference.

Analytical investigations

Defect-free beam

At the outset, it must be stated that the author's team did not have any problem in identifying a system where computer generated response information was used. This clearly indicates that the failure of SI-based approaches to identify a system rests on the response information measured during experiments and has nothing do to with the mathematics of the inverse transformation process used in the system identification. As will be discussed in more detail in the next section – 'Laboratory investigations', a steel beam with a uniform cross-section of 3.81 cm wide, 0.64 cm thick, and 91.0 cm long was used in the laboratory investigation. The same beam was also used in the analytical investigation. Both fixed ended and simply supported beams were tested in the laboratory. Experiments with fixed ended beam are specifically reported here. Similar information on the simply supported beam is reported in Vo and Haldar[10]. The optimal number of elements required to represent the beam was found to be six[16]. All six elements have an equal length of 12.7 cm. Rayleigh damping constants of $\alpha = 7.844$ and $\beta = 2.469 \times 10^{-5}$ obtained by conducting experiments as discussed in the next section are used to generate analytical response information. Analytical modal responses were generated using ANSYS[17], a commercially available finite element program. The beam was excited by a sinusoidal load of $f(t) = 0.15 \sin(100\pi t)$ applied at Node 3, located 25.4 cm from the left hand support as shown in Figure 1. The stiffnesses of all the elements were identified using the transverse $\ddot{\mathbf{y}}(t)$, $\dot{\mathbf{y}}(t)$, $\mathbf{y}(t)$ and angular $\ddot{\theta}(t)$, $\dot{\theta}(t)$, $\theta(t)$ dynamic responses at all nodes. The identified moduli of rigidity of all the elements are shown in Table 1. They are found to be very similar to each other and also similar to the theoretical value of 160.3 Nm^2, as discussed in the next section.

Defective beam

To identify defects in a beam, two defects are introduced in element 2 as shown in Figure 2. They are pictorially shown in Figure 3. The defects are uniformly cut across the width of the beam's top surface and both defects have the same size: 3.2 mm wide and 3.94 mm deep. The

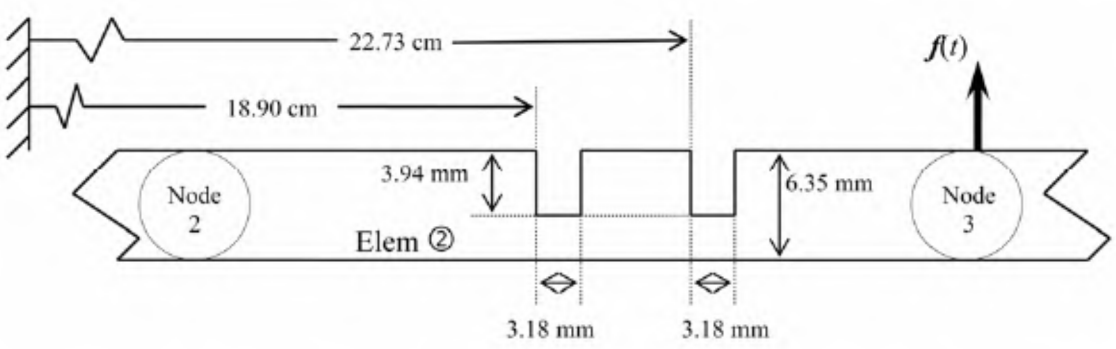

Figure 2. Defects in element 2.

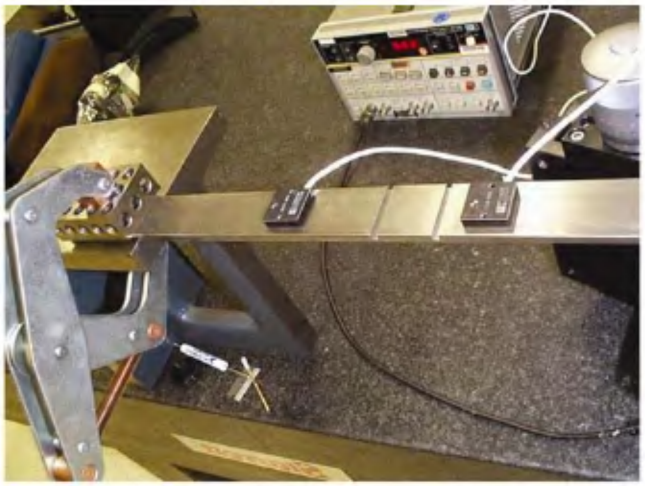

Figure 3. Induced defects.

defects are positioned between nodes 2 and 3, at 18.9 and 22.7 cm from the left support. For the analytical investigation, the defects are modelled by adding two nodes for each cut; one on each side of the defect. These four additional nodes for two cuts create two defective elements of reduced thickness compared to the initial thickness of the beam. The responses at these additional nodes are not used to identify the defects.

The defective beam is again excited by the same sinusoidal load discussed earlier applied at Node 3 and theoretical responses are evaluated using ANSYS. Again, using the theoretical response information, the modulus of rigidity of the elements is identified. The results are summarized in Table 1. Several important observations can be made from the identified results. The modulus of rigidity for element 2 reduced by about 54% from the theoretical value, the maximum amount for all the elements indicating the defects may be in it.

The exercises clearly indicate that the algorithm will identify a defect-free and defective structure when theoretical response information is used. The author's team also showed that systems can be identified using theoretical response information artificially contaminated with noise[2,11]. The study confirms that there is nothing wrong in the theoretical basis in the inverse transformation technique, a major element in the SI-based approaches. To validate or reject Maybeck's comments, an experimental investigation is necessary and several issues in the measurement of responses need broader scrutiny. It is an important but often overlooked area by the theoretical scholars. This is discussed next.

Laboratory investigations

Test specimen

A uniform cross-sectional cold rolled structural steel beam with a precut length of 3.66 m, 3.81 cm wide and 0.64 cm thick was obtained from Phoenix Metals. The beam was machined into 0.91 m sections to use as test articles. The vendor-provided literature indicated that the beams had an elastic modulus of 200,100 MPa, Poisson's ratio of 0.27 and a material density of 8.03 g/cm^3. However, before conducting any test, actual material, stiffness and damping characteristics of the specimens were determined.

In-place properties of the test specimens

Modulus of rigidity: For verification purpose, it is important to know the in-place properties of the test specimens. To evaluate the stiffness of the beam, a Starrett mechanical dial indicator with a resolution of 2.5 μm was used to measure the maximum static deflection of the beam when a 1 kg weight was slowly applied at the midspan of the beam[10]. The average of measured maximum deflections for the simply supported beams was measured to be 555 μm. Using the information on the section properties of the beams and measured deflections, the average elastic modulus is calculated to be 197,340 MPa and not vendor provided value of 200,100 MPa. This measured average elastic modulus value is used in the subsequent discussion. Thus, the corresponding modulus of rigidity (EI) of the beams is estimated to be 160.3 Nm^2.

Damping: The logarithmic decrement method was used to determine the amount of damping present in the beams[18]. In this method, the damping is estimated by measuring the rate of decay of beams' free oscillatory response. To generate the free oscillatory response, a 1 kg dead weight was hung at the beam mid-span and then abruptly removed. A linear accelerometer mounted at mid-span captured the beam's response. The accelerometer data was recorded and stored in the data logger, which was programmed to trigger once the acceleration value changed by 3% from the initial static 1 g (g = acceleration due to gravity = 9.81 m/s^2) level. This feature is very useful for dynamic testing since the beam's response must be sampled instantaneously at the moment the impulse is applied. For consistency, all data in the damping test were sampled at 4000 Hz, the same sample rate used in the dynamic testing.

The free oscillatory motion of the beam was measured in mV. The decaying oscillatory motion of the fixed ended beam was observed to have a natural frequency of approximately 54 Hz. Using the logarithmic decrement method, the damping coefficient ζ, expressed in term of the percent of the critical damping can be estimated as[18]:

$$\zeta \approx \frac{1}{2\pi n} \ln \frac{x_0}{x_n} \tag{1}$$

where x_0 is the amplitude of first cycle and x_n the amplitude after n cycles have elapsed. Using eq. (1), ζ value was estimated to be 1.6% for the fixed ended beams. This damping value was used to calculate the Rayleigh damping coefficients α and β (ref. 8).

Rayleigh damping, $\mathbf{c}_e$, is proportional to mass and stiffness matrices and can be expressed as:

$$\mathbf{c}_e = \alpha\, \mathbf{m}_e + \beta \mathbf{k}_e \tag{2}$$

where α and β are the mass and stiffness proportional constants respectively. These constants have close-form relationship with the first two natural frequencies (f_1 and f_2) of the beam[18]. If ζ_1 and ζ_2 are the damping ratios in the first two modes, they can be shown to be:

$$\zeta_1 = \frac{\alpha}{2\omega_1} + \frac{\beta\omega_1}{2}, \tag{3}$$

and

$$\zeta_2 = \frac{\alpha}{2\omega_2} + \frac{\beta\omega_2}{2} \tag{4}$$

where $\omega_1 = 2\pi f_1$ and $\omega_2 = 2\pi f_2$, and ω_1 and ω_2 are the first and second natural frequencies in rad/s respectively. Assuming $\zeta_1 = \zeta_2$, the following equation is arrived at

$$\frac{\alpha}{4\pi f_1} + \beta\pi f_1 = \frac{\alpha}{4\pi f_2} + \beta\pi f_2. \tag{5}$$

For known values of f_1 and f_2, and using eq. (5), the damping constants α can be expressed in terms of β. Using eq. (3) and the measured damping coefficient, ζ_1, another relationship between α and β can be obtained. Thus, these relationships will give the values for α and β. The first two natural frequencies of the fixed ended beam were experimentally found to be 54 and 145 Hz respectively. The corresponding natural frequencies for the simply supported beam are 25 and 99 Hz respectively.

Test equipment

The team tested defect-free and defective fixed-ended and simply supported beams to address the topics of discussion of this article. A typical test setup for the fixed ended undamaged beam is shown in Figure 4. To carry out the basic experiments, the team used a portable computer configured with an analog-to-digital (A/D) data acquisition board, accelerometers, and an autocollimator. Capacitive sensing accelerometers made by Silicon Designs, Inc., Model 2210-005 were used in the tests. Autocollimator is a device to measure dynamic angular motion. Autocollimator model 431-XY made by United Detector Technology was used for the experiments. After the accelerometers and autocollimator were mounted to the pre-selected node points and the data acquisition set up, the beams were excited several ways and the dynamic responses were measured. The measurements were sampled simultaneously. All instrumentation used in the experiments went through calibrations traceable to the National Institute of Standards and Technology (NIST). The measured acceleration data were successively integrated to obtain the corresponding velocity and displacement time histories. The computer was loaded with the SI

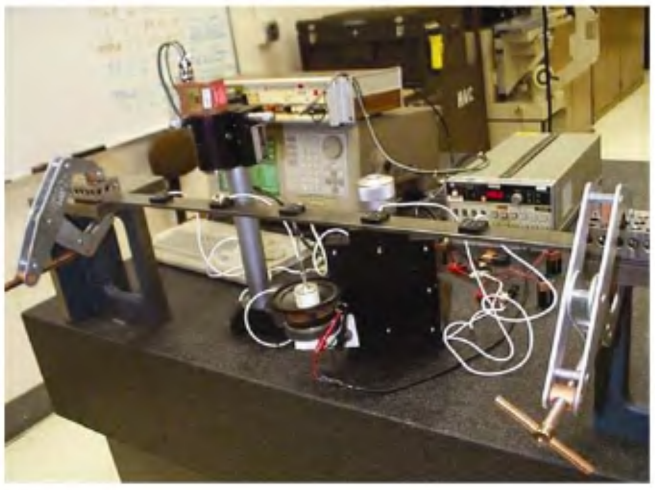

Figure 4. Test setup.

algorithm. As mentioned earlier, the beam was represented by six elements. The task was to identify stiffness properties of all six elements only measuring acceleration time histories for few seconds. Since all the sources of disturbances cannot be eliminated during the experiments, it is important to limit duration of measured acceleration time histories to a minimum, preferably less than a second, to minimize the chances of contamination.

Beam experiments

As shown in Figure 4, five accelerometers were bonded on top to the beam at an equidistance of 12.7 cm apart. The beam was excited at Node 3 (25.4 cm from the left hand support) as shown in Figure 1, by a sinusoidal load of frequency 50 Hz. The fundamental frequency of the fixed ended beam was about 54 Hz. By exciting near its resonance, higher response amplitude of the beam was obtained to keep the signal-to-noise ratio to an optimal level. This practice is not recommended for actual structures because it can damage the structures or the instrumentations.

The accelerometers' analog outputs are sampled, digitized and stored using the Tektronix A/D data logger. A sampling rate of 4000 samples per second was used in capturing the response data throughout the experiment. This high sampling rate assures that aliasing error will not occur in the test data. It also mitigates the integration error in post processing of the test data, as discussed here.

Post-processing of the accelerometer data

Measured acceleration time history may contain many sources of error including noise, high frequency content, slope, and DC bias. All of them may not be present in all recorded acceleration time histories. Since acceleration time histories are integrated to obtain velocity and displacement time histories required for the proposed method, it is important that all the errors are removed for the recorded data. Vo and Haldar[19] discussed in great detail how to remove them efficiently and effectively. Post-processing procedures in the study are briefly discussed here for the sake of completeness.

The first step in post-processing the raw data is converting from millivolts to acceleration unit (m/s^2) by multiplying the accelerometer raw data with the calibrated scale factor. Next, an eighth order Butterworth low-pass filter is applied to the normalized data with a cutoff frequency setting at 120 Hz. Then, the data is normalized about the zero mean to remove the DC bias and the integration error. The transverse velocity and displacement time histories were then obtained by integrating the filtered acceleration data twice; after each integration operation, a second order low-pass filter with a cut off frequency at 10 Hz is applied to the data. This is necessary to remove the integration residual errors; without the low-pass filter, the response velocity and displacement will not be symmetric.

Error in numerical integration is an important element in post processing acceleration time histories, and it needs some additional discussion. Several numerical integration methods such as the trapezoidal rule, Simpson's rule, and Boole's rule were considered by Vo and Haldar[19]. The midpoint rule and other open Newton–Cotes rules were not considered because these rules do not consider the end points. The consequence for not using the end points is the relative phase shift errors occurred as the signal is being integrated. Vo and Haldar[19] demonstrated that even though the trapezoidal rule produces the largest integration error compared to other methods, it is preferred over other rules for the problem under consideration, because of its simplicity and efficiency in computing time.

Evaluation of the elemental stiffness parameter

To generate dynamic responses, the beam was excited at 25.4 cm from the left support with a harmonic excitation. The beam is discretized into six elements. Using the post-processed measured responses and the algorithm developed by the author's team, the stiffness of all the elements are identified. The identified moduli of rigidities are not similar to the expected values as observed in analytical investigation and some of them gave negative stiffness indicating that the method failed to identify the beam[10], confirming Maybeck's statements that a system cannot be identified using measured response information, even when the response information was post-processed as discussed earlier. An exhaustive study was initiated to identify the causes of the non-convergence and is discussed in the next section.

Possible reasons of failure to identify a system

Since measured acceleration time histories recorded by the accelerometers are used to identify a system, sources of error including noise, data latency, scale factor, cross coupling error, and relative phase error among different accelerometers are specifically evaluated.

Noise

Noise is generally considered to be the main reason of non-convergence. After data reduction, it was found that the worst case root-mean-squared (RMS) noise was 0.3% for the accelerometer and 1.7% for the autocollimator. To assess whether noise is the main cause of the non-convergence, the slightly higher RMS noise values of 0.4% and 1.9% were generated and added to computer simulated noise-free data for transverse (accelerometer)

and angular (autocollimator) responses respectively. The noise-polluted responses were then used as input to predict the modulus of rigidities of all the elements. The SI method successfully predicted the elemental rigidities for both noise-free and noise-polluted responses[10]. This eliminates noise as the main cause of non-convergence.

Scale factor and cross coupling errors of accelerometers

Scale factor: Each accelerometer comes with a calibration sheet in which the manufacturer (Silicon Design) provides a scale factor to convert the accelerometer's output voltage into acceleration in terms of *g* units. The typical scale factor for accelerometers used in this experiment is about 800 mV/g. Each accelerometer also has a typical scale factor error of ±2%, caused by calibration errors and nonlinearities.

Cross coupling error: Cross coupling error is primarily caused by mechanical misalignments of the sensing element mounted inside the accelerometer's case. The typical cross coupling error for this accelerometer model is ±2% according to the manufacturer's specifications. The combined root-sum-squared (RSS) error for scale factor error and cross-coupling, denoted hereafter as the amplitude error is ±2.8% ($\sqrt{0.02^2 + 0.02^2} = 0.028 = 2.8\%$. This total RSS error was then added to the transverse (accelerometer) and angular (autocollimator) noise-free theoretical responses obtained by the computer for fixed ended beam. Note angular and transverse responses have the same amount of error, since the angular response is scaled directly from the transverse response, as will be discussed in this section. To determine the convergent threshold for the identification, various levels of the amplitude error, i.e., 0.5, 1.0, 2.0, 3.0 and 4%, were introduced to the computer generated noise-free data. Using the noise-polluted response information, the rigidities of all the elements were identified.

The algorithm converged only when the amplitude error is 0.5% indicating the threshold for the error[20]. When the response amplitudes at all node points were decreased or increased by 4%, the algorithm converged and identified correct rigidities[20]. From the results it can be concluded that the algorithm is not sensitive to the changes in the absolute response amplitude as long as the relative amplitudes between the nodes remain unchanged. Since the total amplitude error is 2.8% and the threshold for the algorithm is only 0.5%, it must be one of the major reasons of non-convergence.

Phase shift error

There are two separate sources of error that cause relative phase shift in the measured responses. The primary source of phase shift error is the integration of the measured acceleration. The worst case phase shifts for velocity and displacement responses are estimated to be 1.8 and 6.5 degrees respectively[10,20]. The second source of phase shift error is data latency that is caused by the sampling rate of the Tektronix data logger. This error occurs because there is a time delay in the sampling of two consecutive responses. The data logger model used in the test has a maximum latency of one microsecond. For the fixed ended beam experiment, there are five consecutive channels to be sampled, one for each accelerometer. This translates to a total latency of 5 microseconds. Given the beam's response at 50 Hz, the 5 microsecond data latency results in a phase shift error of 5×10^{-6} 1/(1/50)(360) = 0.09°. This phase shift is two orders of magnitude smaller than the phase shift error caused by the integration process.

To assess whether the phase shift error is one of the main causes of the algorithm's non-convergence, a maximum RSS phase shift errors of 1.8 degrees for velocity and 6.5 degrees for displacement were randomly generated by computer and introduced to both velocity and displacement noise-free theoretical responses. Using the noise-polluted response information, all the elements of the beam were identified.

The results indicate that the proposed algorithm is very sensitive to the phase shift error in the measured responses. For instance, if the relative phase shift error between responses is 0.5 degree, the algorithm will converge. When the phase shift error is greater than 4.0 degrees, the algorithm failed to converge[10,20]. Clearly, the phase shift of 1.8 and 6.5 degrees for velocity and displacement responses respectively are the other main causes of the non-convergence.

In summary, the proposed algorithm was found to be very sensitive to the amplitude and phase shift errors. These errors need to be mitigated before identifying a structure using the proposed algorithm.

Phase shift error mitigation

In comparing both the measured and computer generated response time histories, it can be observed that transverse and angular responses of the same node are linearly proportional to each other, i.e., they have the same phase and shape but different amplitudes for the experiments conducted in this study. This proportionality is true for all nodes. This suggests that the angular response can be scaled from the transverse response. The angular-to-transverse scaling ratio can be found by dividing the standard deviation of the angular response to that of the transverse response as[10]

$$R = \frac{\sigma_{\text{ang}}}{\sigma_{\text{trans}}}, \tag{6}$$

where R is the angular-to-transverse scaling ratio, σ_{trans} and σ_{ang} are the standard deviations of the transverse and angular responses respectively.

Prior to performing the actual dynamic tests, the angular-to-transverse scaling ratio at each node was determined by a series of tests. The beam was excited at the same point (Node 3) as it would be in the actual dynamic test. Both transverse and angular responses were measured simultaneously by the accelerometer and autocollimator at a given node. Every time the test was performed at the new node, the autocollimator was relocated to measure the angular response at that new node. The same test was repeated for all nodes. Using the measured responses and eq. (6), R values were calculated and results are summarized in Table 2 for the fixed ended beam. Note that the negative scaling ratios indicate that angular response is 180 degrees out of phase relative to transverse response at that node.

Once the ratios are determined, the angular responses no longer need to be measured, because they now can be scaled directly from the measured transverse responses. The same scaling ratio at an individual node is used to derive angular acceleration, velocity and displacement based on the transverse responses measured of the same node. For comparison purposes, both scaled and actual angular acceleration responses measured are plotted and observed to be almost identical to that of the measured angular response[20]. This confirms that the scaling method is accurate for the experiments conducted in this study. Another advantage of using the scaled angular response is that both transverse and angular responses have zero phase error. This feature can be used to mitigate phase induced amplitude error, as will be discussed in this section.

One way to mitigate the phase shift error is use as few independently measured transverse and angular response information as possible. Similar to angular-to-transverse scaling, the transverse responses can be scaled from the transverse response of a single reference node to demonstrate the feasibility of this technique. The reference node can be chosen arbitrarily; however, for this study the reference node and the excitation node are the same. The transverse-to-transverse scaling is different from the angular-to-transverse scaling. The transverse-to-transverse scaling ratio, T, can be found by dividing the standard deviation of the measured transverse response at the reference node (σ_{ref}) to the measured transverse response at the ith node to be scaled (σ_i) as[10,20]

$$T = \frac{\sigma_{ref}}{\sigma_i}. \tag{7}$$

Scaling of the transverse responses is necessary to eliminate relative phase shifts among nodal responses. All responses should have zero phase error once the angular-to-transverse and transverse-to-transverse scaling are applied to the data. One practical advantage of this alternative approach is that the beam is only subjected to the dynamic test once. In this test, all nodal responses are measured and stored, so that they can be post-processed later without interfering with normal operation of the in-service structure.

Table 2. Measured scaling ratios for the undamaged simply supported beam

Ratio	Angular-to-transverse (θ_i/y_i)	Transverse-to-transverse (y_i/y_i)
Node 3/Node 2	0.1276	0.3819
Node 3/Node 3	0.0869	1.0000
Node 3/Node 4	–0.7683	1.2099
Node 3/Node 5	–0.1008	0.9163
Node 3/Node 6	–0.1126	0.3374

Amplitude error mitigation

In actual testing, each transverse and angular response is embedded with amplitude error from the scale factor and cross coupling errors. By using fewer nodal responses, the effect of the amplitude error can be reduced. As a result, the algorithm can tolerate a larger amplitude error in a single response measurement.

To further explore this amplitude error mitigation approach, the six-element beam excited at Node 3 discussed earlier is considered again. The original method requires five nodal responses as input for the fixed ended beam and seven nodal responses for the simply supported beam. The alternative approach requires only two nodal responses for the fixed ended beam and four for the simply supported beam. Two additional responses for the simply supported beam are angular responses at the beam's supports.

Based on the measured transverse response at Node 3 (which is used as reference), the angular-to-transverse and transverse-to-transverse ratios relative to other nodes were calculated using eqs (6) and (7) respectively. Node 3 is chosen as the reference node for developing the scaling ratios, as shown in Table 2. Based on these ratios, the scaled transverse and angular responses were constructed based on the transverse response measured at Node 3. To check the convergence, nodal responses were embedded with the worst case of amplitude errors to identify the modulus of rigidity of all the elements. The algorithm converged indicating the successful mitigating efforts. One drawback of this approach is that the predicted stiffness of elements may not predict the absolute stiffness of the beam. However, for the undamaged beam, they will remain almost the same.

In summary, the amplitude error can be mitigated by using fewer nodal responses and the phase error can be mitigated by scaling all responses based on the measured transverse response of a reference node.

Table 3. Identified stiffness of elements of simply supported beam

Configuration	Elements	Modulus of rigidity (EI) – undamaged (Nm^2)	Modulus of rigidity (EI) – damaged (Nm^2)	Percent changes
Case 1: Responses at nodes 3 and 2	K12	125.4	101.0	–19
	K23	125.6	77.2	–39
	K37	128.0	136.9	+7
Case 2: Responses at nodes 3 and 4	K13	138.9	96.9	–30
	K34	142.0	148.9	+5
	K47	148.3	151.8	+2
Case 3: Responses at nodes 3 and 5	K13	160.4	102.5	–36
	K35	186.7	185.3	–1
	K57	156.9	158.0	+1
Case 4: Responses at nodes 3 and 6	K13	1142.0	704.7	–38
	K36	927.2	873.2	–6
	K67	399.6	376.6	–6

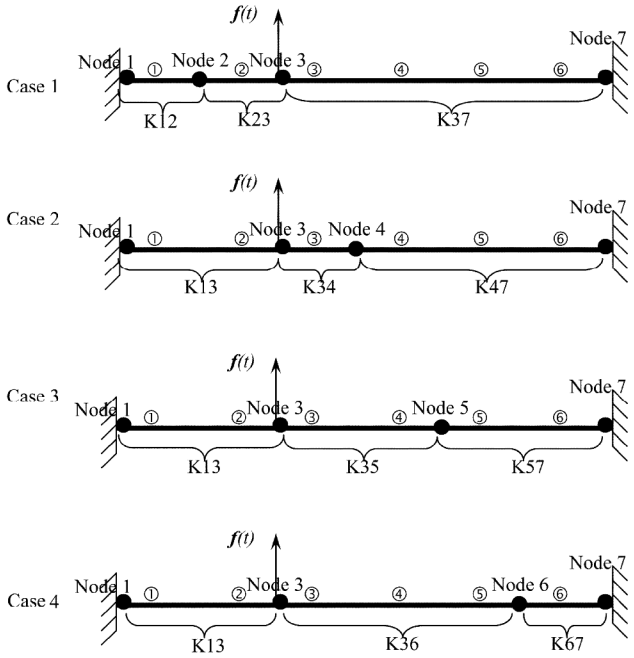

Figure 5. Identification of the beam after phase shift and amplitude error mitigations.

For the fixed ended beam under consideration, the angular responses at all nodes are scaled based on the transverse responses. Obviously, nodes 1 and 7 are expected to have zero transverse and angular responses. Post-processing techniques discussed earlier were used to measured time histories. For the fixed ended beam, two out of a total of five nodal responses (nodes 2 through 6) are selected for the identification purpose. Since Node 3 is considered as the reference node, considering it as one of the two, four different pairs of node points, i.e., (i) nodes 3 and 2; (ii) nodes 3 and 4; (iii) nodes 3 and 5; and (iv) Nodes 3 and 6, as shown in Figure 5, are possible. The identified modulus of rigidity (EI) value for the four cases for the undamaged and damaged beams are summarized in Table 3. Note that the lengths of the elements have changed as shown in Figure 5. In all four cases, the damaged element was correctly identified. The study was successfully extended to identify a two-dimensional steel frame using measured response information[2–4] to demonstrate that the suggested mitigation efforts work for different types of structural systems. The method is yet to be verified in identifying health for real large complex structural systems. There could be other sources of error.

Based on the work completed so far, the study conclusively concludes that a system can be identified using measured response information if the amplitude and phase shift errors are mitigated properly. The presence of noise may not be the most important reason of the non-convergence of the SI-based structural health assessment approaches. Comments made by Maybeck[1] in 1979 may not be valid in 2009.

Conclusions

Structural health assessment techniques using system identification-based approaches have generated a considerable amount of multidisciplinary research interest at present. However, in 1979, Maybeck stated that the inverse transformation technique could not identify a system with measured response information. Presence of many sources of error including noise, data latency, high frequency content, slope, DC bias, etc. in the measured response information were considered to be the major reasons. However, removing these sources from the measured responses may not be adequate to eliminate the non-convergence problem. In this article, it is conclusively demonstrated that a system can be identified if the amplitude and phase shift errors embedded in the meas-

ured responses are mitigated properly. The noise may not be the primary reason for the non-convergence.

Despite the large measurement errors in the sensors (accelerometers and autocollimator) that restricts the use of large number of nodal responses; the algorithm under development by the author's team is robust enough to identify a real system. The SI-based approaches are very sensitive to the accelerometer scale factor, cross coupling, and phase shift errors. These errors in the measured responses were overlooked in the past. Methods to mitigate these errors are discussed here. It is believed that in the near future, when more accurate and affordable sensors become available, the limitation in sensor's accuracy will no longer be a restriction and the method can be expanded to a new level. It is to be noted that that the author and his team studied large complex structures only in analytical investigation. They considered simple beams and two-dimensional frames in the laboratory investigation. The conclusions made are primarily based on the analytical and limited experimental works completed by them. The health assessments of large complex structures in the laboratory and field conditions are yet to be completed. There could be other sources of error. However, the experience gained from the past studies indicates that the system identification-based structural health assessment techniques have unlimited application potential.

1. Maybeck, P., *Stochastic Models, Estimation, and Control*, Academic Press, UK, 1979.
2. Martinez-Flores, R., Katkhuda, H. and Haldar, A., A novel health assessment technique with minimum information: verification. *Int. J. Performability Eng.*, 2008, **4**, 121–140.
3. Haldar, A., Martinez-Flores, R. and Katkhuda, H., Crack detection in existing structures using noise-contaminated dynamic responses. *Theor. Appl. Fracture Mech.*, 2008, **50**, 74–80.
4. Katkhuda, H. and Haldar, A., A novel health assessment technique with minimum information. *Struct. Cont. Health Monitor.*, 2008, **15**, 821–838.
5. Wang, D. and Haldar, A., System identification with limited observations and without input. *J. Eng. Mech., ASCE*, 1997, **123**, 504–511.
6. Kalman, R. E., A new approach to linear filtering and prediction problems. *J. Basic Eng., Trans. ASME*, 1960, 35–45.
7. Hoshiya, M. and Saito, E., Structural identification by extended Kalman filter. *J. Eng. Mech., ASCE*, 1984, **110**, 1757–1770.
8. Ling, X. and Haldar, A., Element level system identification with unknown input with Rayleigh damping. *J. Eng. Mech., ASCE*, 2004, **130**, 877–885.
9. Vo, P. H. and Haldar, A., Health assessment of beams – theoretical formulation and analytical verification. *Struc. Infrastruc. Eng.*, 2008, **4**, 33–44.
10. Vo, P. H. and Haldar, A., Health assessment of beams – experimental verification. *Struc. Infrastruc. Eng.*, 2008, **4**, 45–56.
11. Wang, D. and Haldar, A., An element level SI with unknown input information. *J. Eng. Mech. Div., ASCE*, 1994, **120**, 159–176.
12. Nasrellah, H. A., *Dynamic State Estimation Techniques for Identification of Parameters of Finite Element Structural Models*, Doctoral thesis, Department of Civil Engineering, Indian Institute of Science, Bangalore, 2009.
13. Kerschen, G., Worden, K., Vakakis, A. F. and Golinval, J. C., Past, present and future of nonlinear system identification in structural dynamics. *Mech. Syst. Signal Process.*, 2006, **20**, 505–592.
14. Sohn, H., Farrar, C. R., Hemez, F. M., Shunk, D. D., Stinemates, D. W. and Nadler, B. R., *A Review of Structural Health Monitoring Literature: 1996–2001*, Los Alamos National Laboratory, USA, 2003.
15. Doebling, S. W., Farrar, C. R. and Prime, M. B., A summary review of vibration-based damage identification methods. *The Shock and Vibration*, 1998, **30**, 91–105.
16. Vo., P. H., Haldar, A. and Ling, X., A time-domain system identification technique with optimum number of finite elements. 9th International Conference on Applications of Statistics and Probability (ICASP9-2003), **1**, 481–486.
17. ANSYS version 5.7.2001. The Engineering Solutions Company.
18. Clough, R. W. and Penzien, J., *Dynamics of Structures*, McGraw-Hill Inc, 1993, 2nd edn.
19. Vo, P. H. and Haldar, A., Post processing of linear accelerometer data in system identification. *J. Struct. Eng.*, 2003, **30**, 123–130.
20. Vo, P. H. and Haldar, A., *Experimental Study of the Time Domain Damage Identification*, Report No. CEEM-03-001, Department of Civil Engineering and Engineering Mechanics, University of Arizona, Tucson, Arizona, 2003.